

Study of screwed bamboo connection loaded parallel to fibre

Malkowska, D., Trujillo, D., Norman, J. & Toumpanaki, E

Published PDF deposited in Coventry University's Repository

Original citation:

Malkowska, D, Trujillo, D, Norman, J & Toumpanaki, E 2023, 'Study of screwed bamboo connection loaded parallel to fibre', *Construction and Building Materials*, vol. 398, 132532. <https://doi.org/10.1016/j.conbuildmat.2023.132532>

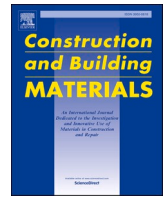
DOI 10.1016/j.conbuildmat.2023.132532

ISSN 0950-0618

ESSN 1879-0526

Publisher: Elsevier

© 2023 The Author(s). Published by Elsevier Ltd. This is an open access article under the CC BY license (<http://creativecommons.org/licenses/by/4.0/>).



Study of screwed bamboo connection loaded parallel to fibre

Dominika Malkowska^{a,*}, David Trujillo^b, Eleni Toumpanaki^a, James Norman^a

^a University of Bristol, UK

^b Coventry University, UK

ARTICLE INFO

Keywords:

Bamboo connections with screws and metal plates
Ductility and fracture in screwed bamboo connections
Bamboo dowelled connections

ABSTRACT

A method for connecting unfilled natural bamboo was proposed, comprising screws and metal plates. The method is commonly used in timber connections, yet in bamboo connections screws are rarely seen, mostly due to the perceived risk of splitting. This study aimed to assess the applicability of screws in bamboo through extensive testing of short-term laterally loaded connection parallel to fibre, including variation of several parameters. An existing timber model was found to be appropriate to estimate the connection yield capacity. In terms of the environmental benefits, connection capacity, stiffness and ductility, the method appears to be an attractive alternative to the common mortar-infilled bolted bamboo connection. The risk of splitting was found to be low provided appropriate spacing parallel and across fibre between screws is provided. The main outcome of the study is the design guidance for the proposed connection, including spacing rules and prediction of the connection capacity.

1. Introduction

Interest in bamboo has been growing over recent years as the construction industry and governments look for ways to reduce their carbon footprint in the face of climate change. Bamboo, just like timber, has the ability to capture and store atmospheric CO₂, but unlike timber it grows at a high speed, with only about 5 years required for the culm (bamboo stem) to reach the full maturity [1]. Hence, provided the bamboo comes from a sustainably managed plantation, and the structure is designed with durability in mind, bamboo structures if used locally can considerably reduce the anthropogenic carbon footprint compared to other construction methods [2].

Bamboo culms are hollow inside and the wall thickness is relatively small. This feature, along with the fibres running in one direction only, significantly hinders connection design, and although many connection methods have been developed, their standardisation is limited.

Dowelled connections are one of the most popular ways to connect bamboo culms. For the purpose of this publication dowelled connections refer collectively to connections with dowel-type fasteners, including dowels, bolts, screws, nails and similar. The typical bamboo dowelled connection includes a single bolt between 8 and 16 mm in diameter that penetrates two or more culms (Fig. 1). The inside of the internode (space between the diaphragms) where the bolt is placed is commonly filled

with cement mortar for additional strength and to prevent splitting from being the governing failure mode. Although the connection is ubiquitous, an analytical model has been developed only recently [3].

Traditionally, the use of screws in natural bamboo has been unpopular due to the prevailing belief that such a connection would inevitably cause splitting. While splitting is commonly observed in nailed connections due to the increase in tangential stress arising upon the nail insertion (Fig. 2), the mechanics of a pre-drilled or self-drilled screwed connection is quite different. Self-drilling screws, unlike nails, do not displace the material but cut it out with the thread while being drilled-in. When predrilling is used, most fibres are similarly cut, and not displaced. This fundamental difference creates a promising hypothesis that screwed connections in fact may not be as brittle as widely considered.

Screwed bamboo connections could have several benefits. Firstly, assuming the connection would replace the traditionally used bolted connection, it would be mortar free. Cement mortar, which infills the internode of bolted connections has been proven to have a high carbon footprint, with cement production being responsible for 7% of all carbon dioxide generated by the energy sector [4]. Secondly, a hypothetical screwed connection would include various small-diameter (less or equal to 6 mm) screws. Unlike in bolted connections with a single fastener, screwed connection with several connectors enhances robustness against splitting (as required by ISO 22156:2021 [5]), i.e. the ability of the connection to redistribute load in the case of an unforeseen loss of

* Corresponding author.

E-mail addresses: dominika.malkowska@bristol.ac.uk (D. Malkowska), david.trujillo@coventry.ac.uk (D. Trujillo), eleni.toumpanaki@bristol.ac.uk (E. Toumpanaki), james.norman@bristol.ac.uk (J. Norman).

<https://doi.org/10.1016/j.conbuildmat.2023.132532>

Received 6 March 2023; Received in revised form 8 May 2023; Accepted 14 July 2023

Available online 20 July 2023

0950-0618/© 2023 The Author(s). Published by Elsevier Ltd. This is an open access article under the CC BY license (<http://creativecommons.org/licenses/by/4.0/>).

Main Notations			
a_1	spacing between fasteners along fibre	s	standard deviation of sample
a_2	spacing between fasteners across fibre	t	fastener penetration depth
a_3	loaded end distance	t_b	bamboo wall thickness
d	fastener diameter	t_s	steel plate thickness
d_{drill}	predrilled hole diameter	F_{ax}	withdrawal capacity
d_{ef}	effective fastener diameter	F_p	predicted capacity
d_{nom}	nominal fastener diameter	F_t	tested capacity
d_r	screw root diameter	F_v	shear capacity
f_{ax}	withdrawal parameter	F_y	yield capacity
f_h	embedment strength	K_{ser}	connection stiffness
f_u	steel wire tensile strength	M_y	fastener bending capacity
m	mean value of sample	N	sample size
n	number of fasteners	μ	ductility
n_{ef}	effective number of fasteners	ρ_{12}	density adjusted to 12% moisture content
		MC	moisture content

one or more individual fasteners. Thirdly, screwed connections, especially with self-drilling screws, are expected to be easier and cleaner to manufacture than traditional bolted connections as no mortar is required. It is also anticipated that screwed connections, if designed correctly, can be as ductile and stiff or better than bolted connections; such an observation was made in Yang et al. [6] for connections comprising steel and engineered timber. Ductility, which is a measure of a structure’s ability to undergo large deformation before the strength loss, is especially important for structures built in earthquake-prone zones, which is often where bamboo is used. Since most failure modes of bamboo members are brittle, connections are often the only source of ductility within a structure. It is also anticipated that screwed connections can be fairly stiff due to the tight fit between the fastener and bamboo. Stiffness is especially important for structures where too much connection slip impacts the ability of the structure to transfer the loads as it was designed, e.g. in trusses. Finally, screwed connections compared with mortar infilled bolted connections also have the advantage of easier disassembly, were the structure to be relocated. An example of a screwed connection with metal plate is shown in Fig. 3.

Although standardization of bamboo is still in an early stage, recent developments led to the publication of ISO 22156:2021 [5], ISO 19624:2018 [7], and ISO 22157:2019 [8], which currently are the most comprehensive suite of standards for bamboo design, grading and testing, respectively. The design standard [5] provides equations for dowelled connections, including screws. The applicability of the standard is discussed in Malkowska et al. [9], where it was shown that for single nailed bamboo connections the code equations are conservative. The equations contained in ISO 22156:2021 [5] cover embedment failure of bamboo under dowel, splitting failure and plug shear (or



Fig. 2. Splitting in nailed connection (Coffee region, Colombia).

shear-out) failure, while the contribution from fastener bending is excluded. The standard does not provide any spacing rules, so its usefulness for multiple-fastener connections is limited.



Fig. 1. Examples of bamboo bolted connections (Coffee region, Colombia).



Fig. 3. Example of a screwed bamboo connection with metal plate (Coffee region, Colombia).

Because of the similarities between bamboo and timber, bamboo is often studied using models developed for timber. The European Yield Model (EYM), first proposed by Johansen [10], is one of the most widely used dowel connection models in timber. The model has been adopted in several design codes, including in Eurocode 5 (EC5) [11]. The model covers timber to timber and steel to timber connections. For the purpose of this publication only single shear steel to timber connections will be discussed. The EYM theory is based on equilibrium of bending moments and shear forces acting on the dowel and distinguishes between various failure modes depending on the plate thickness (Fig. 4), where *thin* plate is defined as of thickness less or equal to half dowel diameter, and *thick* plate as of thickness larger or equal to dowel diameter. The EYM predicts ductile failure, i.e. either embedment failure of the timber, or combination of the embedment failure and the fastener failure. For staggered connections loaded parallel to grain, brittle failure (timber splitting) is assumed to be covered by adequate spacing rules, and for connections arranged in line along the grain, by using an effective number of fasteners n_{ef} . For connections loaded perpendicular to grain, in addition to the EYM model, EC5 provides a fracture energy equation predicting splitting capacity.

Studies on connections with small-diameter fasteners in natural

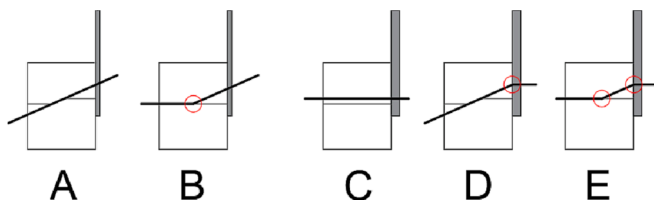


Fig. 4. Failure modes for single shear steel to timber connections: A-B: *thin* plate, C-E: *thick* plate, plastic hinge circled.

bamboo are sparse. Trujillo and Malkowska [12] investigated embedment strength and stiffness of nailed connections and withdrawal capacity of screwed connections in *Guadua* bamboo, and proposed empirical equations for the studied parameters. Harries et al. [13] assessed experimentally the withdrawal capacity of various screw types in *Moso* bamboo and observed that the results were not affected by the screw insertion method, i.e. self-drilling or predrilling, and that *Moso* appears to have higher withdrawal capacity than *Guadua*. Malkowska et al. [9] showed that the EYM model is applicable to nailed bamboo connections with *thin* steel plates loaded parallel to fibre, whereas Kou et al. [14] tested a relatively small sample of single-fastener screwed bamboo to bamboo and bamboo to steel connections loaded parallel to fibre and developed a theoretical model including the effects of the screw head and thread. Zhou et al. [15] tested a sleeve nailed bamboo connection in flexure and found that the connection significantly reduced bending capacity of the connected beams due to brittle failure at the connection.

To this end, due to the promising hypothesis about the behaviour of screws in bamboo and limited research on the subject, this study aims to further develop the understanding of dowelled connections in unfilled bamboo internodes, through an experimental and theoretical analysis of screwed connections. The following research expands the previous study on nailed connections in bamboo [9].

2. Testing methodology

The testing comprised 248 shear tests on screwed steel-bamboo connections, with varying number of up to five countersunk-head and up to four pan-head screws arranged in line or staggered across the fibre direction. The bamboo species used was commercially supplied *Phyllostachys edulis* (commonly known as Moso). The culms were stored in the Structures Testing Lab of the Queens Building at the University of Bristol in an environment with relative humidity in the range of 18 – 44% and temperature 21 – 26 °C, measured with a data logger for 2 weeks preceding the start of testing. The moisture content (MC) of each specimen was measured by oven-drying after the test, and the mean value was found to be $9.0 \pm 0.9\%$. The sample density adjusted to 12% moisture content ρ_{12} was $729 \pm 90 \text{ kg/m}^3$.

The specimens were obtained through saw-cutting culms to the required length. Each saw-cut section of the culm accommodated between 4 and 8 tests. The sample included both split-free specimens as well as those with naturally pre-existing splits (fissures) of various depths. The tested connection was located as far as possible from any pre-existing splits in the tangential direction (min 20 mm either side of the fastener). There were no pre-existing splits along the fibre where the connection was located.

The tested connection was placed at one end of the bamboo specimen. The other end was fixed to the testing machine with a 5-mm-thick steel plate and a number of screws, always higher than the number of screws in the tested connection. The displacement was applied to the specimen through the fixing plate that was clamped in the machine. The steel plate of the tested connection was clamped directly in the machine grip (Fig. 5). The loaded end distance was $12 \times$ nominal fastener diameter ($12d_{nom}$), which follows from the previous study on nails [9]. The specimens were hollow inside, i.e. without any infill material. The specimen wall thickness was measured at each fastener location after the test.

To eliminate the influence of the steel plate elastic deformation and potential slippage at the fixing connection, a set of two linear variable differential transformers (LVDT) were used to measure displacement of the bamboo specimen and of the tested connection plate (see Fig. 5). The test was carried out using an *Instron* universal testing machine with a 25 kN load cell, and the load was applied in tension (short-term) along the fibre direction at the rate 0.6 mm/min. The loading rate was chosen so that the maximum load was reached no earlier than after 60 s from the test start, which follows from the dowel-bearing test standard

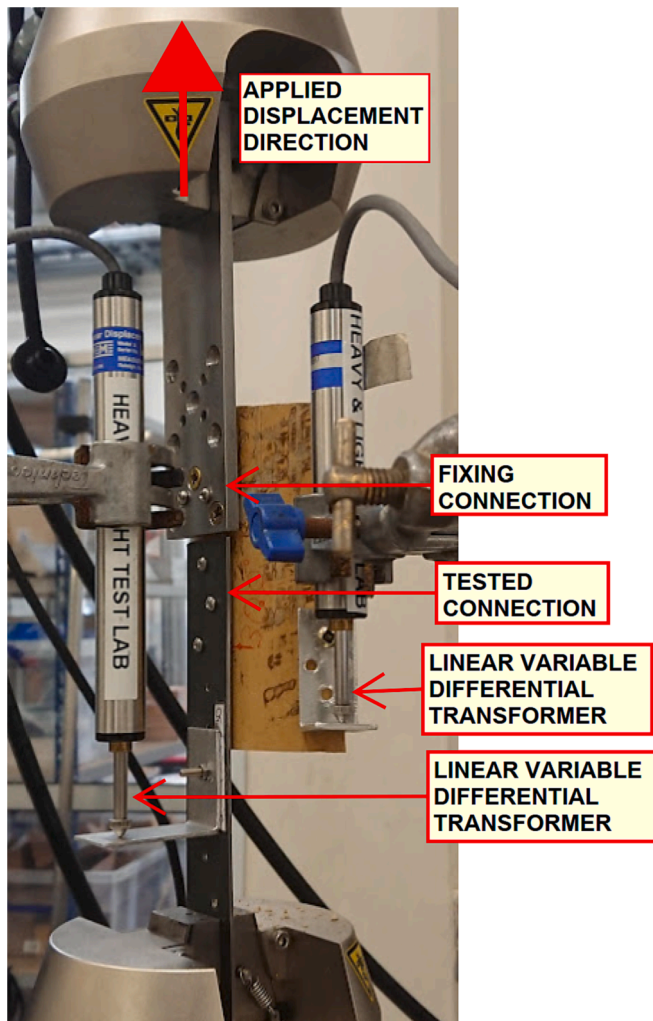


Fig. 5. Test set-up.

ASTM D5764-97a [16] that was used in previous studies on bamboo embedment strength [12 17]. Each tests with pan-head screws was extended until ultimate failure occurred, i.e., load dropped to 80% of its maximum value, according to ISO DTR 21141:2022 [18]. As the countersunk-head screws were expected to be less suitable than pan-

head screws due to their protruding head in *thin* plates, ductility analysis was deemed to be unnecessary and the tests with countersunk-head screws were stopped once the maximum load was reached, i.e. when capacity and stiffness could be assessed.

The tested fasteners included carbon steel and stainless steel screws of diameters: 3.0, 3.5, 4.0 and 5.0 mm with pan or countersunk head. The screws properties are listed in Table 1. The range of steel plate thickness for pan-head screws was: 0.9, 1.5, 2.0, 2.8 mm and for countersunk-head screws 1.9 mm. The testing configurations are listed in Table 2. In the staggered configuration all screws were staggered, i.e. no two screws were placed in the same fibre line. This differs from the EC5 nomenclature, where the staggered configuration includes some connectors placed in the same line along the grain (fibre). In this study the spacing across fibre a_2 was d_{nom} for screws spaced at a minimum distance of a_1 along fibre and $2d_{nom}$ for screws spaced at a minimum

Table 2

Tested configurations: carb - carbon steel, ss - stainless steel, cs – countersunk head, t_s – steel plate thickness, d_r – screw root diameter. Bamboo wall thickness t_b and spacing along fibre a_1 not shown for clarity (large number of configurations).

Screw head type	t_s/d_r	Screw material	Set-up	Number of screws n	Number of tests
pan	≥ 1.0	ss	staggered	3	6
pan	≥ 1.0	ss	staggered	4	8
pan	≥ 1.0	carb	staggered	3	6
pan	≥ 1.0	carb	staggered	4	8
pan	≥ 1.0	carb	in line	2	13
pan	0.5–1.0	ss	staggered	3	7
pan	0.5–1.0	carb	staggered	2	11
pan	0.5–1.0	carb	staggered	3	7
pan	0.5–1.0	carb	staggered	4	8
pan	0.5–1.0	carb	in line	2	21
pan	0.5–1.0	carb	in line	3	7
pan	0.5–1.0	carb	in line	4	9
pan	0.5–1.0	carb	in line	5	4
pan	< 0.5	ss	staggered	2	6
pan	< 0.5	ss	staggered	3	6
pan	< 0.5	carb	staggered	2	20
pan	< 0.5	carb	staggered	3	6
pan	< 0.5	carb	in line	2	8
pan	0.5–1.0	carb	–	1	18
pan	< 0.5	carb	–	1	3
cs	0.5–1.0	carb	in line	2	25
cs	0.5–1.0	carb	in line	3	7
cs	0.5–1.0	carb	in line	4	3
cs	0.5–1.0	carb	–	1	31
				$\Sigma =$	248

Table 1

Properties of the screws, carb - carbon steel, ss - stainless steel, *data from manufacturer (screw too short for testing).

Screw image	Screw type	Material	Nominal diameter d_{nom} [mm]	Root diameter d_r [mm]	Predrilled hole diameter in bamboo d_{drill} [mm]	d_{drill}/d_r	Bending capacity M_y [Nmm]
	Intended for wood	carb	3.0	1.90	1.5	0.79	2600 ± 180*
	Intended for wood	carb	4.0	2.55	1.9	0.75	4500 ± 300
	Intended for wood	carb	5.0	3.15	2.5	0.79	7400 ± 240
	Intended for wood	carb	4.0	2.55	1.9	0.75	4500 ± 300
	Intended for wood	carb	3.5	2.25	1.9	0.84	3400 ± 100
	General purpose	carb	4.0	2.65	1.9	0.72	5330 ± 230
	General purpose	ss	3.0	2.00	1.5	0.75	1500 ± 40
	General purpose	ss	4.0	2.85	2.5	0.88	3800 ± 130

distance of $0.5a_1$ along fibre. The spacing across fibre a_2 was dictated by the gap between the plate and the bamboo for the outermost screw (typical $d_{nom} = 4$ mm) being around 0.6 mm (in connections with 4 screws – the maximum tested number), which based on engineering judgement was deemed to be the maximum acceptable value (Fig. 6). The staggered configuration with more than four screws would imply a larger gap at the outermost screw. The influence of the gap was not investigated, however it is expected it may impact the ability of the screw to bend, which indicates that for connections with more than four staggered screws curved plates would be preferable (Fig. 7).

In each test the screws penetrated fully through the bamboo wall so that the tapered tip was protruding inside the culm. The sample included specimens with various thickness t_b between 6 and 14 mm. The spacing along fibre direction a_1 was in the range of $5d_r - 25d_r$. All tests with countersunk-head screws had screws arranged in one line, and for pan-head screws both arrangements were tested. The holes for pan-head screws were predrilled and the countersunk-head sample included tests with pre-drilled and self-drilled specimens. Self-drilling was found to be difficult for high density specimens and in general it was found easier to predrill the holes instead. The effect of self-drilling was not analysed. The predrilled hole size is specified in ISO 22156:2021 [5] as between $1.1d_r - 1.2d_r$, however in the current study the predrilled holes were smaller, between $0.72d_r - 0.88d_r$ (Table 1). The hole size was determined through trials, starting with smaller holes and increasing their size until the process of drilling-in was deemed to be easy enough while no splitting was observed.

The screw bending moment capacity was assessed for 5 screws of each type in three point bending tests carried out to ASTM F1575 – 03 [19] (Fig. 8a). The embedment strength f_h was assessed in the previous study [9] using smooth dowels (Fig. 8b). The predicting embedment strength equation (Eq. (1)) proposed in the previous study [9] is assumed in the current study to be applicable to screws by substituting the dowel diameter d with the screw root diameter d_r .

$$f_h = -54.43 - 1.33t_b - 3.41d^2 + 28.37d + 0.12 \rho_{12} \quad (1)$$

where f_h [N/mm²], d [mm], t_b [mm], ρ_{12} [kg/m³].

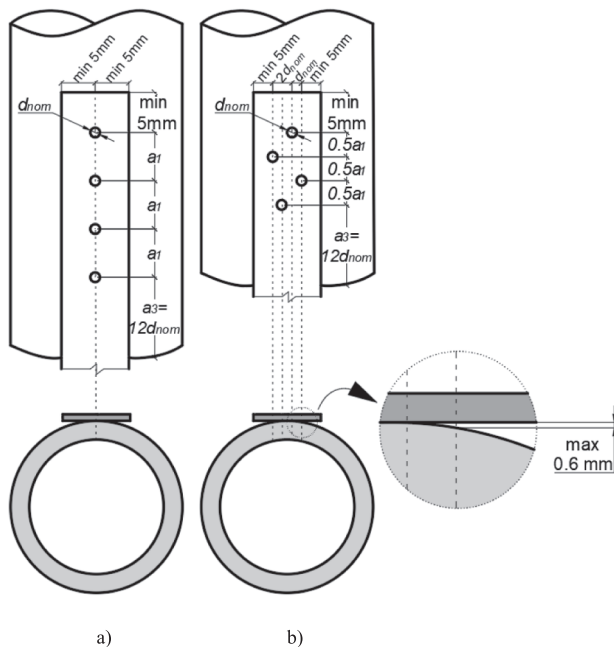


Fig. 6. Schematics of the screw arrangement – example with four screws: a) arranged in a line b) staggered across the fibre direction.

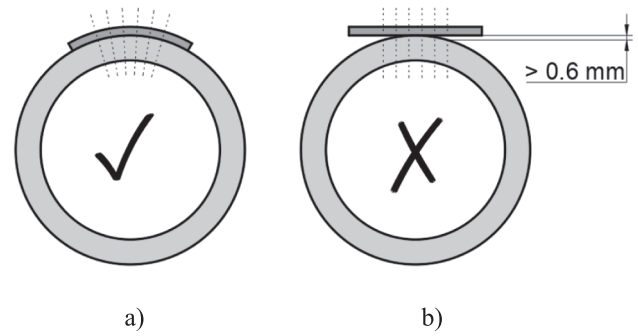


Fig. 7. Schematics of a hypothetical connection with more than four staggered screws: a) curved plate (recommended), b) flat plate (not recommended).

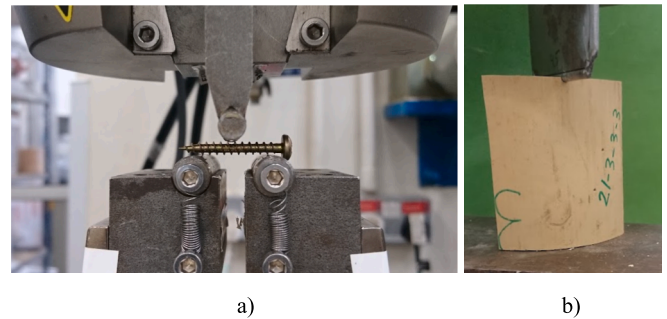


Fig. 8. Material properties testing: a) screw bending capacity, b) bamboo embedment strength.

3. Results and analysis

3.1. Failure modes

Three ultimate failure modes were observed for pan-head screwed connections: screw withdrawal, screw failure and bamboo splitting, whereas for countersunk-head connections, the failure was either withdrawal or splitting (Fig. 9). In some cases multiple failure modes were recorded occurring simultaneously, or one after the other.

The withdrawal failure could be characterized as ductile (gradual unloading). The failure tended to be more pronounced at the top screw (furthest from the loaded end). In the tests with thin plates, withdrawal was co-occurring along with deformation around the plate holes. Splitting was fairly brittle (sudden load drop), which led to a catastrophic failure. The splitting failure was in a form of a single split either at the hole centreline or at the hole edge. In most instances splitting would propagate through the whole length of the connection, including the loaded end. The loaded end was $12d_{nom}$, which follows from studies on nails [9]. The split origin was not investigated. The bamboo shear failure, where two shear cracks form at the hole edges, was not observed. That failure mode would be expected at connections with a small end-distance ($a_3 \leq 3d$) [9]. The screw failure was caused by exceeding screw bending resistance at either the bamboo/plate interface or at the head/plate interface.

3.2. Load-displacement plots

Load-displacement plots for all tests are shown in Fig. 10, where it can be observed that on average countersunk-head screws result in similar ultimate capacity, similar initial stiffness ($K_{ser,int}$) but overall lower stiffness ($K_{ser,fin}$) than pan-head screws. For countersunk-head screws, after reaching the initial rotation capacity (mode A in Fig. 4), the stiffness reduced due to the unrestricted rotation of the head, until

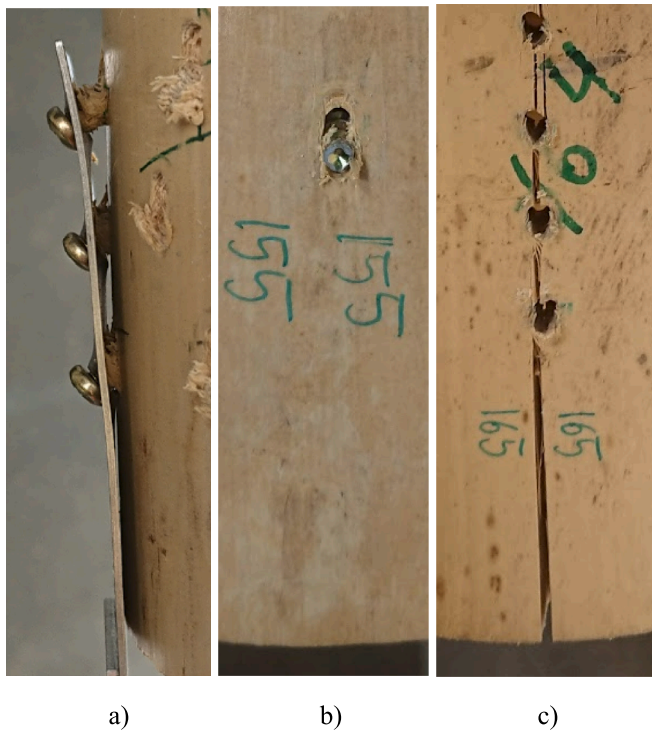


Fig. 9. Examples of observed failure modes: a) screw withdrawal, b) screw failure, c) splitting.

the head touched the plate, by which point the screw interaction with the plate began and either the screw began to bend, the plate around the hole began to deform, or both. Finally, the screws would begin to withdraw unless splitting failure had occurred first. Countersunk-head screws are generally used either in timber where the head can sink into the material or in *thick* plates with countersunk holes. Therefore, the use of countersunk-head screws in bamboo is only recommended in *thick* plates with countersunk holes, where the behaviour is expected to be similar to pan-head screws.

Although efforts were made to avoid any rigid body deformation in the set-up (Fig. 5), slight initial adjustments of the clamped specimen were recorded in some of the tests, which was caused by imperfections in the set-up straightness. The lack of straightness was caused by difficulties in aligning the top and bottom steel plates to ensure that they were in the same plane. The lack of straightness is unavoidable due to

the inherent variability in outer diameters of bamboo culms. As a result, some tests had initial negative displacements, as visible in Fig. 10.

The experimental data was analysed in terms of the connection shear capacity F_v , stiffness K_{ser} and ductility μ , which were determined according to ISO DTR 21141:2022 [18]. The yield point was determined at the intersection of the load–displacement curve and a straight line fitted to the initial linear portion of the graph $K_{ser,int}$ (pan head screws) or the final linear portion of the graph $K_{ser,fin}$ (countersunk head screws) and offset by $0.05d_r$. Ductility (pan head screws only) was calculated as the ratio of the ultimate displacement to the yield displacement. The ultimate displacement corresponded to the ultimate failure load (load drop to 80% maximum value). The connection stiffness $K_{ser,int}$ was estimated from the tangent of the initial linear portion of the load–displacement graph. For the tests where the initial displacement was negative, stiffness was read from the portion of the graph after the set-up adjustment took place.

3.3. Ductility

The analysis in this section refers to pan-head screws only since as discussed, the tests with countersunk-head were only conducted to assess the capacity and stiffness. Several parameters were investigated from which t_s/d_r , a_1/d_r , t_b and screw material were found to be the most relevant for predicting ductility. In Fig. 11, ductility is plotted against t_s/d_r ratio for tests with $n \geq 2$ screws. For tests where the ultimate failure was the screw failure or splitting, ductility appears to increase with increasing t_s/d_r ratio, while withdrawal failure results in high ductility regardless of t_s/d_r ratio, which implies that the observed plastic deformation around plate holes in *thin* plates in the withdrawal mode does not affect ductility. ISO 22156:2021 [5] set the requirements for any joints in load bearing structures to have ductility $\mu \geq 1.25$, and for joints used in the main seismic resisting structures $\mu > 2.5$. For staggered screws, the threshold of $\mu \geq 1.25$ is met for almost all tests, with a few exceptions where $t_s/d_r = 0.3$ or 0.6 , while $\mu > 2.5$ is met for the vast majority of the tests with $t_s/d_r \geq 0.75$. For screws in line, the threshold of $\mu \geq 1.25$ is met for the vast majority of the whole sample, with a few exceptions where $t_s/d_r = 0.6$. The majority of the in line tests fail the threshold of $\mu > 2.5$, with the exception of the tests where $t_s/d_r = 0.45$.

For both staggered and in line configurations, the withdrawal failure appears to be the most common failure mode for lower t_s/d_r ratios and its frequency decreases with increasing t_s/d_r ratio (Fig. 12), while the opposite is true for the screw failure. For staggered screws, splitting was mostly observed at lower t_s/d_r ratios. This is expected, since insufficient t_s/d_r ratio would impede bending of the screw, thus eliminating this screw failure mode, and instead making splitting more likely. For in line

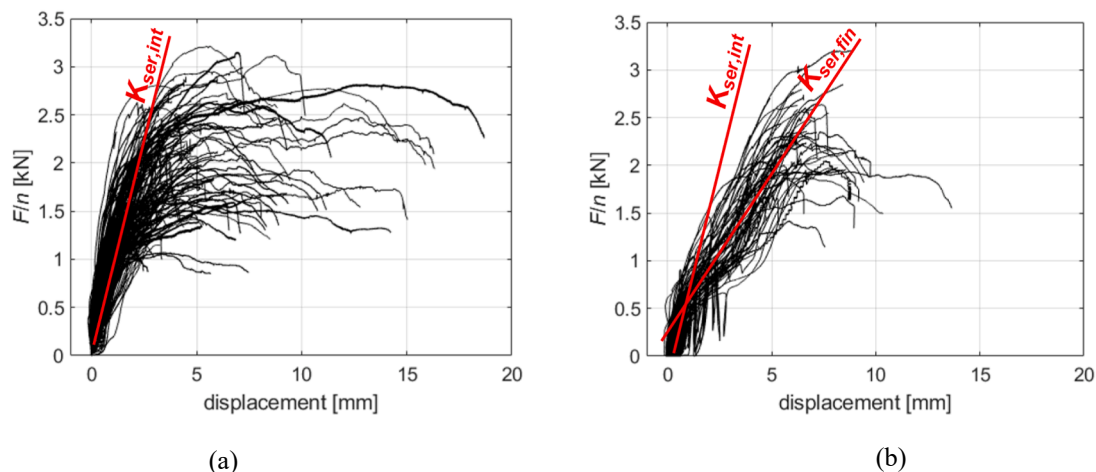


Fig. 10. Load-displacement plots of all tests with a) pan-head screws, b) countersunk-head screws.

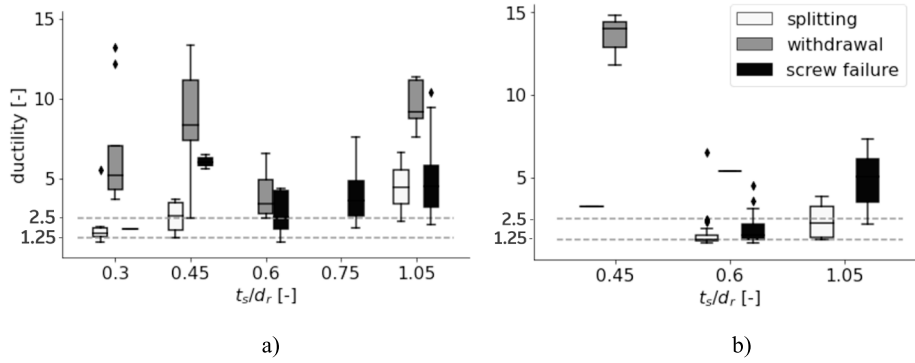


Fig. 11. Ductility versus t_s/d_r ratio, t_s/d_r values averaged into bins for clarity, horizontal lines show ISO ductility thresholds, screws: a) staggered, b) in line.

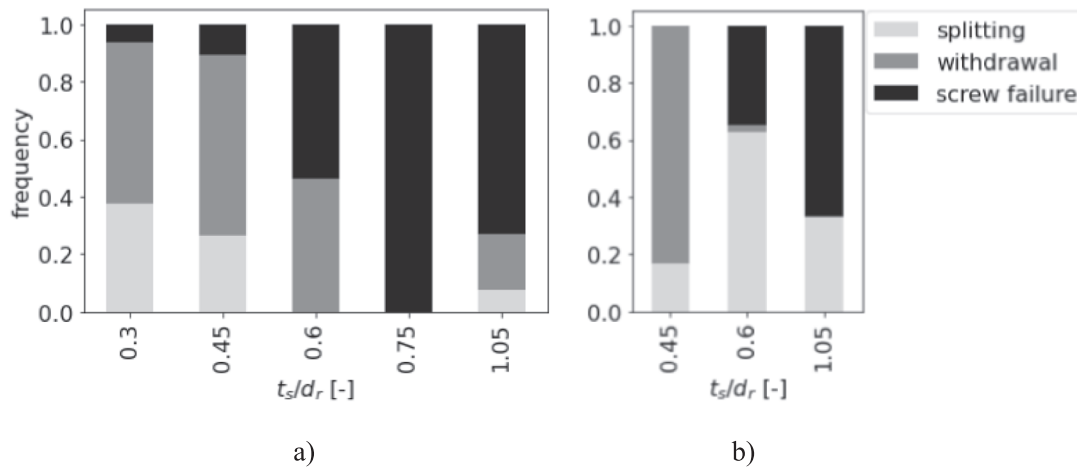


Fig. 12. Failure modes frequency versus t_s/d_r ratio, t_s/d_r values averaged into bins for clarity, screws: a) staggered, b) in line.

screws, the frequency of splitting does not decrease with increasing t_s/d_r ratio (unlike for staggered screws), which can be an indication of the group effect, where the accumulation of stresses causes early splitting (this point is discussed later).

To analyse further, the effect of a_1/d_r ratio was plotted in Fig. 13. For clarity, the plot for in line screws (Fig. 13b) excludes tests with $a_1/d_r = 22$ that were tested with either *thin* ($t_s/d_r < 0.5$) or *thick* plates ($t_s/d_r > 1.0$), since those tests resulted in relatively high ductility, caused by the t_s/d_r ratio and not by the spacing. For staggered screws, the threshold of

$\mu \geq 1.25$ is met for the majority of the sample, while $\mu > 2.5$ is met for almost all tests with larger spacing between screws ($a_1/d_r = 15$). For in line screws a_1/d_r ratio does not affect the ductility, which is much lower than for staggered screws. The threshold of $\mu \geq 1.25$ for in line screws is met for most of the tests, while $\mu > 2.5$ is met for a few tests only.

Ductility was also found to be affected by the screw material, especially in tests with *thick* plates, where ductility was higher for stainless steel compared with carbon steel screws (Fig. 14a). This is expected since in *thick* plates the failure mode tends to be the screw failure, and

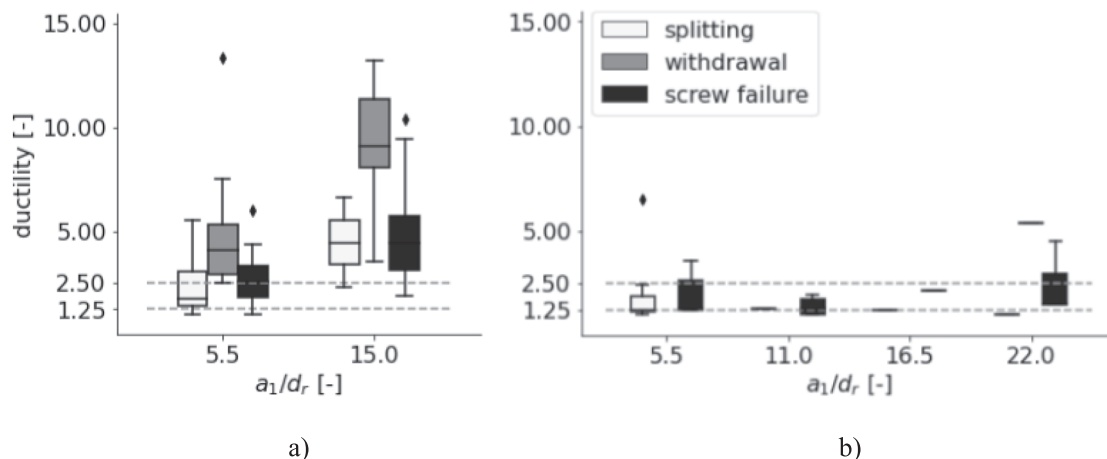


Fig. 13. Ductility versus a_1/d_r ratio, a_1/d_r values averaged into bins for clarity, horizontal lines show ISO ductility thresholds, screws: a) staggered, b) in line.

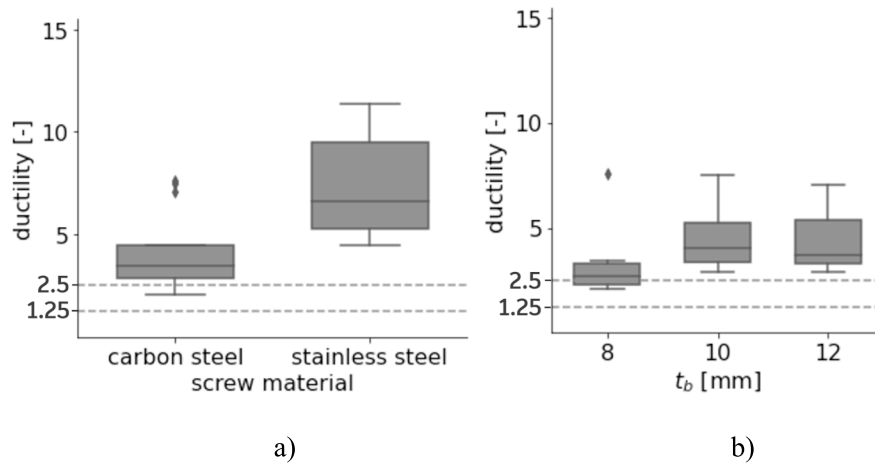


Fig. 14. Ductility (for $t_s/d_r > 1.0$) versus: a) screw material, b) wall thickness (carbon steel screws), t_b values averaged into bins for clarity; horizontal lines show ISO ductility thresholds.

stainless steel in general is more ductile than carbon steel, which was also observed in the screw bending tests (Fig. 15). It was also observed that for carbon steel screws in *thick* plates, ductility is slightly higher for thicker walls (Fig. 14b).

All of the observations discussed were used to classify the ductility values, considering the thresholds of $\mu \geq 1.25$ and $\mu > 2.5$. The result of this classification is presented as separate decision trees for staggered screws (Fig. 16) and in line screws (Fig. 17), where for each leaf the 5th percentile (ranked) and the mean ductility value are denoted as $\mu_{0.05}$ and μ_m , respectively. The number of tests considered at each leaf is noted in parenthesis, e.g. for connections with staggered screws spaced at $a_1/d_r \geq 15$, with $n \leq 4$ and $0.5 \leq t_s/d_r < 1$, there are 9 tests, the 5th percentile ductility value is 1.9 and the mean ductility value is 4.2. ISO 22156 [5] does not specify the confidence level for the ductility thresholds; however; in this study, it is recommended to use the 5th percentile values, similar to how it is done for the strength properties.

3.4. Stiffness

The analysis in this section only refers to pan-head screws since as discussed, countersunk-head screws in *thin* plates result in low overall stiffness (Section 3.1) and are only recommended to be used in *thick* plates with countersunk holes, where the head type is expected not to have an effect on stiffness. For pan-head sample, since no difference in stiffness was observed between in line and staggered arrangements, the two set-ups were not differentiated. ISO 22156:2021 [5] does not provide any requirements for the connection stiffness. It is however an important connection parameter, since excessive slip at the connection may impact the system behaviour, e.g. in trusses.

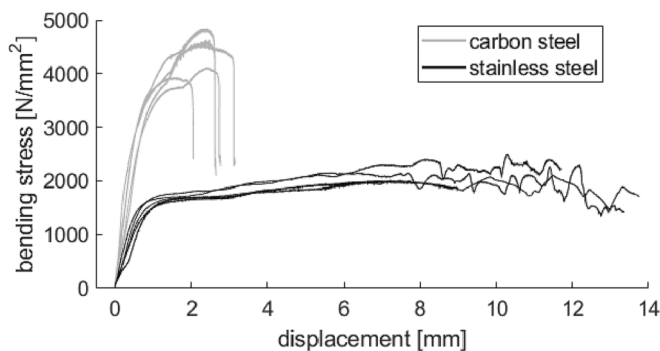


Fig. 15. Bending stress versus displacement for 4-mm-diameter general purpose carbon steel and stainless steel screw.

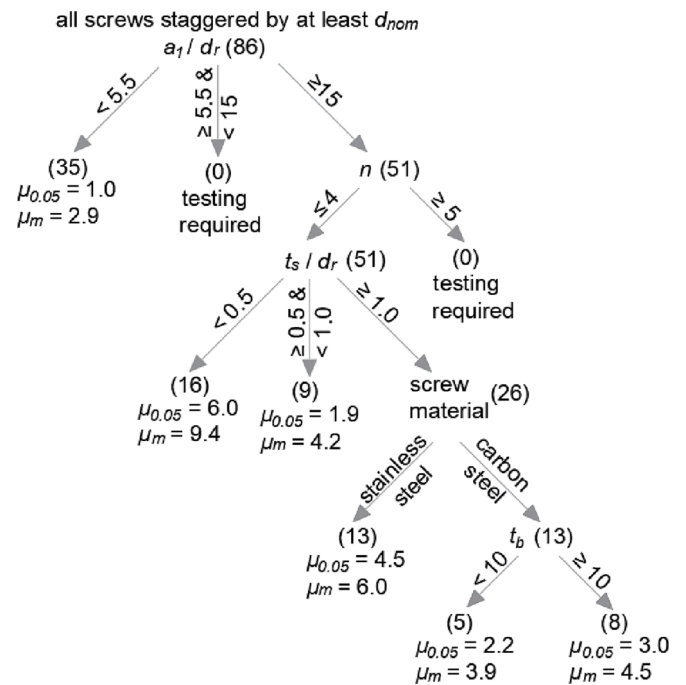


Fig. 16. Decision tree for characteristic and mean ductility considering ISO thresholds – staggered screws, value in parenthesis – sample size, n – number of screws.

The stiffness was plotted against a number of parameters, among which the number of screws in the connection n was found to be the most relevant in predicting the connection stiffness (Fig. 18a). The stiffness increases with increasing number of screws, i.e. average values of $K_{ser,n}$ were found to be 1013, 2510, 3420 and 4160 N/mm, for $n = 1, 2, 3$ and 4 screws in the connection, respectively. The stiffness increase is directly proportional to the fastener count in the connection (n), i.e. fitting of $K_{ser,n} = nK_{ser,1}$ outputs R^2 of nearly 1. The trend of increasing stiffness with increasing fastener count is very promising, since it is expected that a potential connection would include several screws, which results in higher connection capacity and also higher stiffness.

The t_s/d_r ratio does not appear to affect the stiffness (Fig. 18b) most likely due to a tight fit of the screw in the plate hole (plate holes matching d_{nom}) and a tight fit between the screw head and the plate. Had the fit been less tight, the screw head in *thin* plates would be expected to

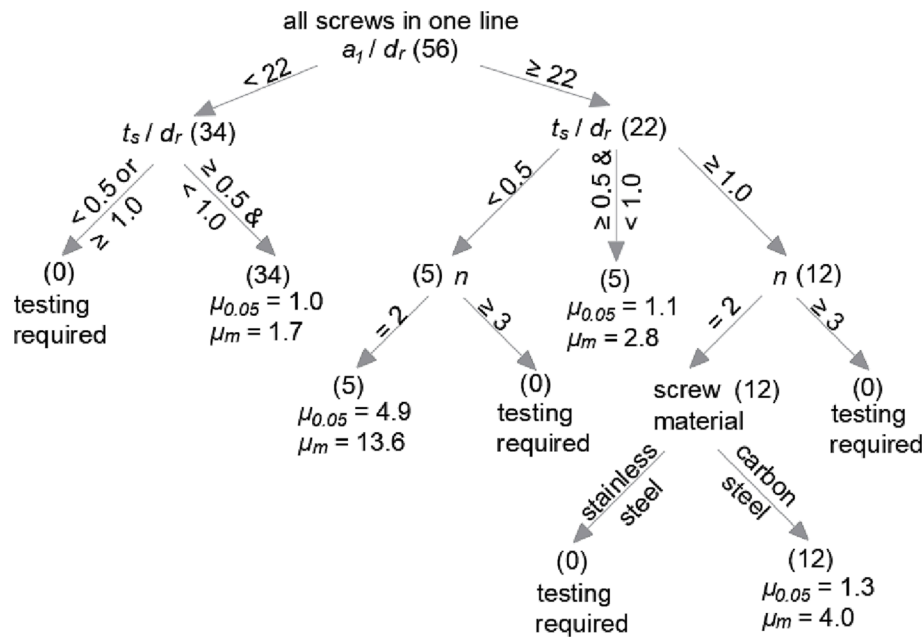


Fig. 17. Decision tree for characteristic and mean ductility considering ISO thresholds – in line screws, value in parenthesis – sample size, n – number of screws.

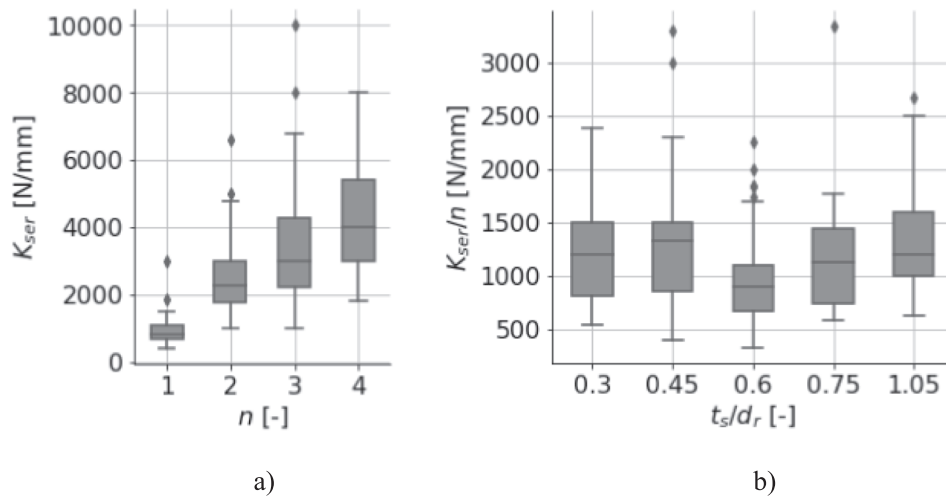


Fig. 18. A) stiffness versus number of screws n, b) Stiffness per screw versus t_s/d_r ratio, t_s/d_r values averaged into bins for clarity.

rotate and result in lower stiffness than in *thick* plates and a similar load–displacement shape as for the countersunk-head screws (Fig. 10b).

3.5. Yield capacity

In the study on nailed steel-bamboo connections [9] it was found that the European Yield Model (EYM), which was developed for timber joints, gives good estimation of the bamboo nailed ductile connection capacity. The bamboo nailed model refers to the failure mode A in Fig. 4 and Eq. (2a), where the fastener rotates but does not bend and the failure is due to exceeded embedment stress. The EYM equations for yield capacity F_y of modes A - E (Fig. 4) are shown in Eq. (2a)–(2e). In EC5 the effect of the screw thread is considered through the effective dowel diameter d_{ef} taken as 10% larger than the screw root diameter d_r and, where the fastener bends, by an additional capacity caused by friction between the shearing members (rope effect), taken as 25% of the fastener withdrawal capacity F_{ax}. The term F_{ax}/4 in Eq. (2a)–(2e) for screws must not exceed 100% of the Johansen’s part of the equation, while for round nails the contribution is limited to 15% and for bolts to

25%. Those assumptions were also implemented in this study. The fastener penetration depth t in Eq. (2a)–(2e) is replaced with bamboo wall thickness t_b in this study, since in bamboo the screw will always penetrate through the whole wall thickness unlike in timber structures, where partial penetration is common.

$$F_y = \min \left\{ \begin{array}{l} 0.4f_h t d_{ef} \\ 1.15 \sqrt{2M_y f_h d_{ef}} + \frac{F_{ax}}{4} \\ f_h t d_{ef} \\ f_h t d_{ef} \left[\sqrt{2 + \frac{4M_y}{f_h d_{ef} t^2}} - 1 \right] + \frac{F_{ax}}{4} \\ 2.3 \sqrt{M_y f_h d_{ef}} + \frac{F_{ax}}{4} \end{array} \right. \quad (2a)–(2e)$$

In general, the observed ductile failure for screws where t_s/d_r ≥ 1 was failure mode D, for screws where t_s/d_r < 0.5 failure mode A, and for screws where 0.5 ≤ t_s/d_r < 1.0 a combination of the two modes. In the

pure failure mode A, the fastener rotates and the rotation is assumed to be resisted only by the material embedment strength, and this was indeed observed in nailed connections in bamboo [9]. In the current study, due to the tight fit of the screw in the plate hole (plate holes matching d_{nom}), and due to the tight fit between the head and the steel plate (pan-head), the screw rotation in plates where $t_s/d_r < 1$, was hindered and could progress only along with the plate deformation around the screw and/or plate bending (Fig. 19).

Although the failure type was found to be dependent on the t_s/d_r ratio, it was found that overall, the failure mode D results in a good prediction for all tests, without differentiating between the t_s/d_r ratio (whenever the failure is not caused by splitting). The good fit of the prediction D for tests that failed in mode A could be explained by the extra resistance from the steel plate (bending and bearing failure around the holes), which added to the embedment strength of the pure mode A. For comparison, both predictions are plotted for tests with various t_s/d_r ranges (Fig. 20), where a relatively good fit of the prediction mode D can be observed, with $R^2 = 0.83$ when all tests are included.

The equations used to make predictions for mode A and mode D failure are Eq. (3) and Eq. (4), respectively. The withdrawal capacity was calculated according to Eq. (5), which was determined experimentally for screws in Moso [13]. The embedment strength in Eq. (3)–(4) was calculated with Eq. (1), substituting d with d_r .

$$F_y = n(0.4f_h t_b d_{ef}) \quad (3)$$

$$F_y = n \left(f_h t_b d_{ef} \sqrt{2 + \frac{4M_y}{f_h d_{ef} t_b^2}} - 1 + \frac{F_{ax}}{4} \right) \quad (4)$$

where $d_{ef} = 1.1d_r$

$$F_{ax} = 30.3 d_{nom}^{0.9} t_b^{1.23} \quad (5)$$

where F_{ax} [N], d_{nom} [mm], t_b [mm].

3.6. Risk of splitting

In the timber dowelled connection theory developed by Jorissen [20] it was proven that the shear capacity of a connection with multiple fasteners arranged in line along the grain direction is not equal to the capacity of a single fastener multiplied by the number of fasteners. Instead, the effective number of fasteners n_{ef} should be used, which is less than the actual fastener number. The reduction is a function of the number of fasteners and spacing between the fasteners. Jorissen [20] concluded that the reason for the reduced capacity is the stress concentration at fastener locations leading to early brittle failure due to exceeded shear and/or tangential tensile capacity in timber. The model

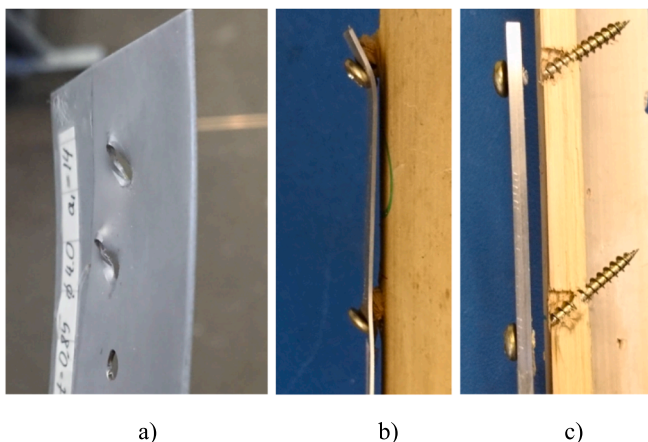


Fig. 19. Typical failure in: a) thin plate – deformation around holes, b) thin plate - plate bending, c) thick plate.

was adopted in EC5, as an indirect prediction of the splitting capacity, since the reduction is applied to the EYM equations, which are based on embedment and bending capacity of the fastener.

According to the EC5 model [11], for nails and bolts the reduction is calculated using Eq. (6) and Eq. (7), respectively.

$$n_{ef,nails} = n^{k_{ef}} \quad (6)$$

where $k_{ef} = 1.0, 0.85, 0.7, 0.5$ for $a_1 \geq 14d, = 10d, = 7d, = 4d$, respectively.

$$n_{ef,bolts} = \min \left\{ \begin{array}{l} n \\ n^{0.9} \sqrt[4]{\frac{a_1}{13d}} \end{array} \right. \quad (7)$$

The influence of the screw number and spacing along the fibre direction for the tests in this study was plotted in Fig. 21 and Fig. 22, respectively. All tests, i.e. including both pan-head and countersunk-head screws are included in this analysis. The F_t/F_p ratio represents the tested to predicted capacity ratio where F_t was taken as yield capacity for tests where yielding was observed and as maximum capacity for tests without yielding (with brittle failure). The predicted capacity F_p was calculated with Eq. (4). A trend can be observed for screw number in connections with screws arranged in line. As expected, and according to timber theory, the ratio decreases with increasing number of fasteners. No trend can be observed for screws staggered across the fibre direction, which is also in accordance with the theory, where the n_{ef} factors only apply to non-staggered fasteners. Small spacing along the fibre for in line and staggered screws also appears to reduce the F_t/F_p ratio, which is in agreement with the design for in line screws according to Eurocode 5 [11]. In timber connections for in line spacing of $> 14d$, no reduction in capacity is expected (Eq. (6)), and this threshold also appears to be applicable to the results for the in line screws in bamboo (Fig. 21a) and is also proposed as a conservative threshold for staggered screws (Fig. 21b), i.e. at spacing $> 14d$, for both in line and staggered screws, no reduction in capacity is expected.

In order to quantify the reduction, the n_{ef} factor was derived through fitting a non-linear model with coefficients C_1, C_2 and C_3 (Eq. (8)). The equation form was chosen to resemble the EC5 equation for bolts (Eq. (7)), which takes into account both spacing and fastener number, and takes the form of:

$$F_{tot} = C_1 n^{C_2} \left(\frac{a_1}{d_r} \right)^{C_3} F_{ind} \quad (8)$$

where F_{tot} – total tested capacity: either yield capacity or maximum capacity where yield was not observed; F_{ind} – predicted capacity of an individual fastener with Eq. (4).

The adjusted coefficient of determination of the fitted function was found to be $R^2 = 0.65$. The fitting resulted in Eq. (9), which can be applied to assess the mean connection shear capacity in Eq. (10). This prediction covers all ductile and brittle failure modes. It should be noted that even though no reduction for the in line screws with $a_1 \geq 14d_r$ is proposed ($n_{ef} = n$), such design may result in unacceptably low ductility (see Fig. 13b).

$$n_{ef} = \begin{cases} 0.86 n^{0.82} \left(\frac{a_1}{d_r} \right)^{0.1} & \text{for } a_1 < 14d_r, \text{ in line screws} \\ 0.84 n \left(\frac{a_1}{d_r} \right)^{0.065} & \text{for } a_1 < 14d_r, \text{ staggered screws} \\ n & \text{for } a_1 \geq 14d_r, \text{ in line screws} \\ n & \text{for } a_1 \geq 14d_r, \text{ staggered screws} \end{cases} \quad (9)$$

$$F_v = n_{ef} \left(f_h t_b d \sqrt{2 + \frac{4M_y}{f_h d_{ef} t_b^2}} - 1 + \frac{F_{ax}}{4} \right) \quad (10)$$

Using Eq. (10) the observed versus predicted capacity for all tests is

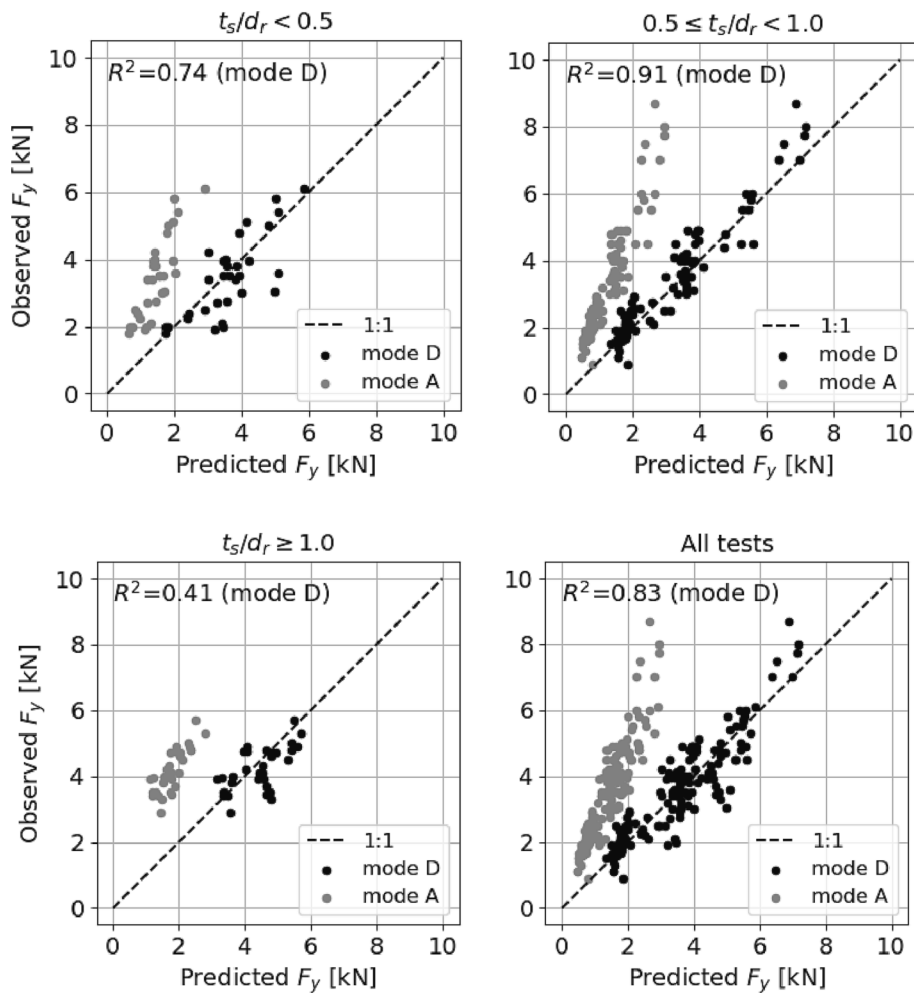


Fig. 20. Observed versus predicted yield capacity for tests with ductile ultimate failure mode.

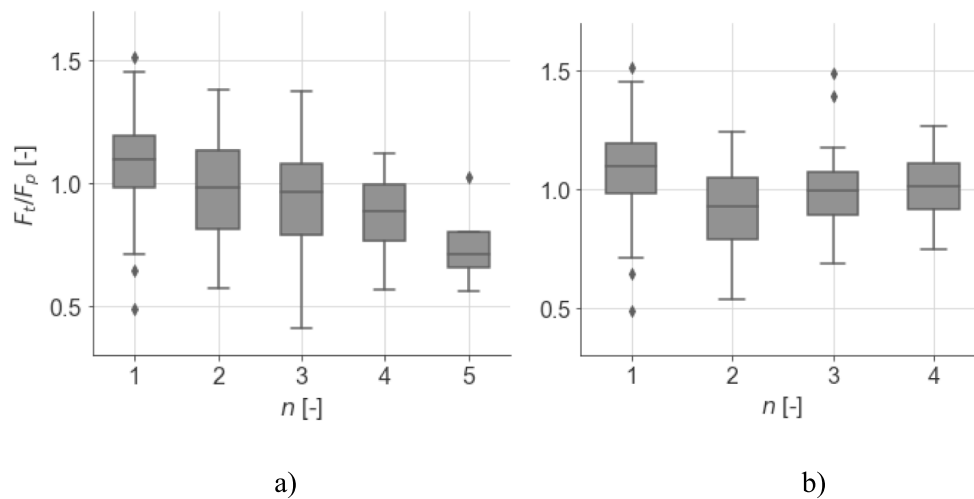


Fig. 21. Tested to predicted capacity ratio plotted against number of screws for all tests, plot for $n = 1$: baseline data, a) in line screws, b) staggered screws.

plotted in Fig. 23a. For comparison, the same equation but with n instead of n_{ef} is plotted in Fig. 23b, where it can be observed that using n_{ef} instead of n improves both R^2 and MSE (mean squared error).

3.7. Characteristic model

The proposed equation (Eq. (10)) is based on mean values. However, for design purposes it should be converted to characteristic values. The estimation of the characteristic value X_k was made according to ISO 12122-1:2014 [21], where X_k is taken as the 5th percentile value with

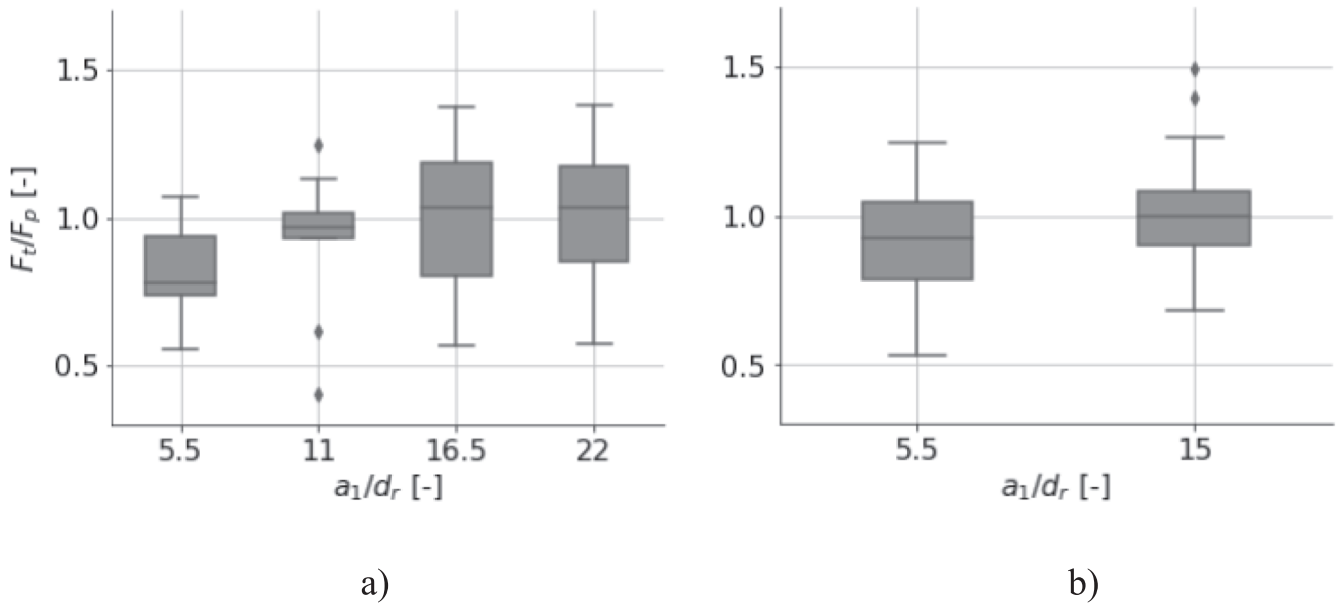


Fig. 22. Tested to predicted capacity ratio plotted against a_1/d_r ratio, a_1/d_r values averaged into bins for clarity: a) in line screws, b) staggered screws.

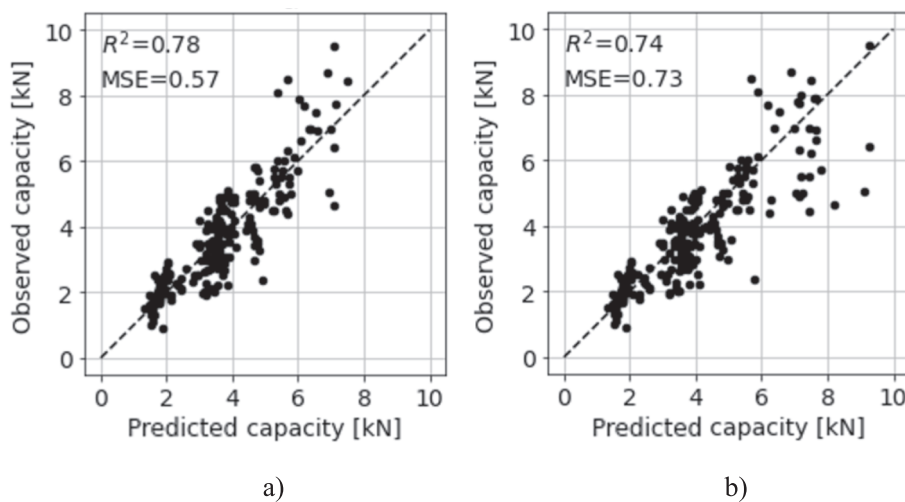


Fig. 23. Observed versus predicted capacity for all tests including all failure modes: a) $n = n_{ef}$, b) $n = n$.

75% confidence — $X_{0.050,75}$, and it is calculated as follows:

$$X_k = X_{0.05, 0.75} = X_{0.05} \left(1 - \frac{k_{0.05, 0.75} \frac{s}{m}}{\sqrt{N}} \right) \tag{11}$$

where: $X_{0.05}$ is the 5th percentile from the test data, $k_{0.050,75}$ is a multiplier based on the number of tests and distribution type, s is standard deviation, m is mean value of the data and N is the sample size (notations adjusted for this publication).

The main material strength properties of the proposed equation are bamboo embedment strength, screw withdrawal capacity and screw bending capacity. The embedment strength equation is a function of another material property – density (Eq. (1)). It was therefore chosen to adjust density ρ_{12} , screw bending capacity M_y and screw withdrawal capacity F_{ax} to the characteristic values. The values $\rho_{12,k}$ and $M_{y,k}$ were found using Eq. (11), assuming the non-parametric method according to ISO 12122-1:2014 [21] since the Kolmogorov-Smirnov goodness of fit test resulted in a poor fit for both normal and log-normal distributions. The value of $F_{ax,k}$ was calculated as $F_{ax,k} = f_{ax,k} d_{ef} t_b$, where $f_{ax,k}$ is a

withdrawal parameter, which was assumed 28.5 N/mm^2 based on values reported by Harries et al. [13]. The equation for $f_{h,k}$ was derived from Eq. (1) but with the value of $\rho_{12,k}$ in place of ρ_{12} (and d_r in place of d). The characteristic shear capacity prediction $F_{v,k}$ takes the form of Eq. (12) and is plotted for all tests in Fig. 24 (in black), where 95% of the data points result in higher observed than predicted capacity.

$$F_{v,k} = n_{ef} \left(f_{h,k} t_b d_{ef} \sqrt{2 + \frac{4M_{y,k}}{f_{h,k} d_{ef} t_b^2}} - 1 + \frac{f_{ax,k} d_{ef} t_b}{4} \right) \tag{12}$$

The characteristic screw bending capacity $M_{y,k}$ if unknown may be assumed as $M_{y,k} = 0.3 \times f_{u,k} \times (1.1d_r)^{2.6}$, taking the minimum tensile strength of the screw material $f_{u,k} = 600 \text{ N/mm}^2$ which follows from EC5. Such an assumption was proved to result in 96% data points with lower observed than predicted capacity, thus meeting the requirements of a characteristic prediction model (plotted in grey in Fig. 24).

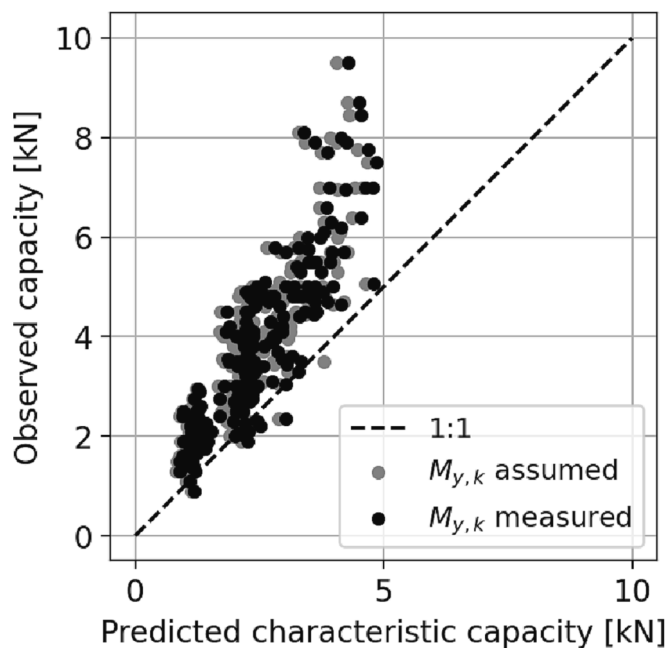


Fig. 24. Tested capacity plotted against predicted characteristic capacity for all tests.

4. Discussion

Since the studied connection is envisaged to be an alternative connecting method to the common bolted connection (Fig. 1), it is of interest to compare their properties. The experimental results indicate that the yield capacity of a screwed connection is around 1.85 ± 0.4 kN per fastener for a typical 4-mm-diameter screw, for both carbon and stainless steel type. Although stainless steel screws have lower bending capacity than carbon steel screws (Table 1), for screws with $d_{nom} = 4$ mm used in this study, the larger root diameter of the stainless steel screws (2.85 mm compared with 2.65 mm for carbon-steel screws) balanced out their lower bending capacity and therefore both screw types resulted in a similar connection yield capacity.

The bolted connection (with mortar infilled internodes) with 15.9-mm-diameter bolt was reported to have around 22 kN tested capacity [3], which is approximately equivalent to 12No 4-mm-diameter screws, i.e. 6 screws at each culm side (two shear planes in total). The connection with smaller bolt ($d_{nom} = 9.5$ mm) was reported to have 12 kN yield capacity [3], which is equivalent to having three/four screws at each culm side. In terms of stiffness, the bolted connection was reported to have stiffness of 3200 N/mm ($d_{nom} = 15.9$ mm) and 2300 N/mm ($d_{nom} = 9.5$ mm) [3]. For screws, as discussed, the stiffness increases with increasing numbers of screws, and therefore it is expected it would be higher when compared with stiffness of a bolted connection (for three screws $K_{ser} = 3420$ N/mm). The average ductility of the bolted connection was reported to be 3.0 ($d_{nom} = 15.9$ mm) and 3.5 ($d_{nom} = 9.5$ mm).

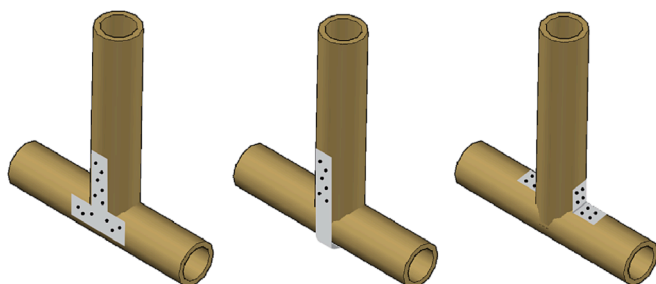


Fig. 25. T-shaped bamboo connection ideas with steel plates and screws.

mm) [3], which is within the range of values recorded for screws in *thick* plates. The ductility could be significantly increased by the use of *thin* plates, which induce withdrawal failure mode.

5. Conclusions

The study showed that the proposed method of using screws and metal plates is viable. The connection capacity can be reliably predicted with an existing timber model. The connection appears to be an attractive alternative to a common mortar-infilled bolted connection. Although no particular design detail has been proposed, it is encouraged to exploit the possibilities arising from the study findings in terms of a potential connection design. Some possible designs of a T-shaped bamboo connection using steel plates and screws are shown in Fig. 25.

The provided guidance only applies to connections loaded parallel to fibre. For connections loaded perpendicular to fibre, the capacity may be assessed with a fracture model derived by Malkowska et al. [22]. Even though the model in [22] was derived based on a single bolted connection, the fracture theory used in the model implies that the predicted capacity is expected to be applicable for any dowel connection type. More studies are encouraged to verify this assumption. The withdrawal strength can be assessed with models proposed in the literature, e.g. [12] for Guadua and [13] for Moso bamboo.

While designing a potential screwed connection, it must be noted that the premise of environmental benefits from the use of screws and metal plates as connectors in bamboo is only true if the amount of steel is minimized. This should be considered when choosing the plate thickness, screw spacing and overall geometry of the connection, which will dictate the plate overall size.

Main findings from the study:

- Shear capacity of a screwed connection can be predicted with a model developed for timber.
- Shear capacity is affected by the spacing along fibre (staggered and in line screws) and the number of screws in the connection (in line).
- Staggering screws is the most important factor for ductility.
- Stainless steel screws result in higher ductility than carbon screws in connections with *thick* plates.
- Connection stiffness increases linearly and proportionally to the number of screws, at least up to 4 screws (the maximum tested number).
- Tight fit between the screw head and the plate is essential for stiff connections.
- If sufficient spacing is provided between the screws along fibre and all screws are staggered, splitting is rare and the failure mode of connections with *thin* plates tends to be screw withdrawal, and with *thick* plates — screw failure.
- The screw failure tends to be brittle for plates between *thin* and *thick*, and ductile for *thick* plates.
- Inserting screws without predrilling can be laborious for high density (thin wall) specimens.
- Low ductility is caused by either splitting or screw failure.
- Average yield capacity of a 4-mm-diameter screw was found to be 1.85 ± 0.4 kN and average stiffness 1 kN/mm.

CRedit authorship contribution statement

Dominika Malkowska: Conceptualization, Formal analysis, Investigation, Methodology, Writing – original draft, Writing – review & editing. **David Trujillo:** Conceptualization, Methodology, Writing – review & editing. **Eleni Toumpanaki:** Conceptualization, Methodology, Writing – review & editing. **James Norman:** Conceptualization, Funding acquisition, Methodology, Writing – review & editing.

Declaration of Competing Interest

The authors declare that they have no known competing financial interests or personal relationships that could have appeared to influence the work reported in this paper.

Data availability

Data will be made available on request.

Acknowledgement

The first author acknowledges the support of EPSRC (EP/R513179/1).

References

- [1] V. Göswein, J. Arehart, C. Phan-huy, F. Pomponi, G. Habert, Barriers and opportunities of fast-growing biobased material use in buildings, *Build. Cities* 3 (1) (2022) 745–755.
- [2] L. Kuehl, K. Yiping, Carbon Off-Setting with Bamboo. International Network for Bamboo and Rattan. INBAR, Beijing, PR China, 2012.
- [3] J.F. Correal, E. Prada, A. Suárez, D. Moreno, Bearing capacity of bolted-mortar infill connections in bamboo and yield model formulation, *Constr. Build. Mater.* 305 (2021) 124597.
- [4] Infrastructure and Energy Alternatives, LLC, “Energy Technology Perspectives 2020,” 2020.
- [5] International Organization for Standardization, “ISO 22156:2021 - Bamboo structures — Bamboo culms — Structural design,” 2021 .
- [6] R. Yang, H. Li, R. Lorenzo, M. Ashraf, Y. Sun, Q. Yuan, Mechanical behaviour of steel timber composite shear connections, *Constr. Build. Mater.* 258 (2020) 119605.
- [7] International Organization for Standardization, “ISO 19624:2018 - Bamboo structures — Grading of bamboo culms — Basic principles and procedures,” 2018.
- [8] International Organization for Standardization, “ISO 22157:2019 - Bamboo structures - Determination of physical and mechanical properties of bamboo culms - Test methods,” 2019.
- [9] D. Malkowska, J. Norman, D. Trujillo, Theoretical and experimental study on laterally loaded nailed bamboo connection, *Constr. Build. Mater.* 342 (2022) 127971.
- [10] K. Johansen, Theory of Timber Connections, International Association for Bridge and Structural Engineering Publications, 1949.
- [11] European Committee for Standardization, Eurocode 5: Design of Timber Structures, BSI, Brussels, 2004.
- [12] D.J.A. Trujillo, D. Malkowska, Empirically derived connection design properties for Guadua bamboo, *Constr. Build. Mater.* 163 (2018) 9–20.
- [13] K.A. Harries, P. Morrill, C. Gauss, C. Flower, Y. Akinbade, D. Trujillo, Screw withdrawal capacity of full-culm *P. edulis* bamboo, *Constr. Build. Mater.* 216 (2019) 531–541.
- [14] Y.-F. Kou, L.-M. Tian, J.-P. Hao, B.-B. Jin, X. A, Lateral resistance of the screwed connections of original bamboo, *J. Build. Eng.* 45 (2022) 103601.
- [15] H. Zhou, Y. Yan, N.a. Su, C. Fang, H. Liu, X. Zhang, B. Fei, X. Ma, Flexural Properties of Multiple Bamboo Beams with Connection Joints, *Forests* 13 (11) (2022) 1851.
- [16] American Society for Testing and Materials, “ASTM D5764-97a - Standard Test Method for Evaluating Dowel-Bearing Strength of Wood and Wood-Based Products,” 2018.
- [17] D. Malkowska, J. Norman, D. Trujillo, Empirically derived embedment strength and fracture behaviour of Moso bamboo. World Conference on Timber Engineering WCTE, 2020.
- [18] International Organization for Standardization, “ISO/TR 21141:2022 - Timber structures — Timber connections and assemblies — Determination of yield and ultimate characteristics and ductility from test data,” 2022.
- [19] American Society for Testing and Materials, “ASTM F1575-03 - Standard Test Method for Determining Bending Yield Moment of Nails,” 2010.
- [20] A. Jorissen, “Double shear timber connections with dowel type fasteners,” PhD thesis, TU Delft, 1998.
- [21] International Organization for Standardization, “ISO 12122-1 - Timber structures — Determination of characteristic values — Part 1: Basic requirements,” 2014.
- [22] D. Malkowska, T. Laux, D. Trujillo, J. Norman, Adaptation of a wood theoretical fracture model for predicting splitting capacity of dowelled connections in bamboo, *Constr. Build. Mater.* 357 (2022) 129358.